Annals of Biomedical Engineering, Vol. 25, pp. 440–451, 1997
Printed in the USA.

0090–6964/97 $10.50 + .00

A Dynamic Model of the Hand with Application in Functional Neuromuscular Stimulation

ALI ESTEKI and JOSEPH M. MANSOUR

Department of Mechanical and Aerospace Engineering, Case Western Reserve University, Cleveland, OH

Abstract—Potential hand function in people with tetraplegia was evaluated using a three-dimensional dynamic mathematical model. The model was used to evaluate hand positioning, grasp force, and the outcome of surgeries such as tendon transfers and joint fusion, in situations typical of those encountered when using functional neuromuscular stimulation to restore function in people with tetraplegia. In the model, the hand is treated as a jointed multibody system. Each joint is subjected to muscle moments, passive joint moment, and moments due to grasp forces. Model simulations showed that function was highly dependent on both muscle strength and joint passive moments. The potential for tendon transfers, such as the Zancolli-lasso and intrinsic-plasty, to improve hand function was demonstrated, but their value is subject-dependent. It was also shown that activation of multiple thumb muscles (adductor pollicis, abductor pollicis brevis, and flexor pollicis longus) without interphalangeal joint fusion can provide convenient lateral pinch posture with ~70% more grip force than a currently used method, which includes joint fusion but requires only one muscle. Finally, a grasp protocol was introduced and shown successful in palmar grasp and hold of movable cylindrical objects using only extrinsic muscles, provided the fingers could be extended sufficiently to enclose the object.

Keywords—Hand modeling, Hand function, Interaction of passive and active moments, Tip pinch, Lateral pinch, Reciprocal motion.

INTRODUCTION

Functional neuromuscular stimulation is a developing technology that restores limited voluntary control of skeletal muscles where nervous system damage has rendered them paralyzed (19,20,25). Using functional neuromuscular stimulation, a person with tetraplegia can reach, grasp, and pick up an unmodified object and manipulate it for use, independently. Such movements are complex, requiring the use of multiple muscles controlling multiple segments, connected by multiple joints.

One means for better understanding the interaction of muscles, segment motion, and an object and, thus hand function, is through a dynamic model of the hand. Several static models (7,17,21,28) and, to a lesser extent, dynamic models of hand function (6,8) have been developed and used to predict grip strength, tendon excursion, hand posture, and the ability to grasp objects with limited groups of muscles, although, with few exceptions, their use has been limited to normal hand function. Kinetic models have revealed that dynamic torque associated with finger movements can be large in relation to joint torque produced by muscles, especially in faster movements (11,14). Electromyographic measurements and torque patterns associated with finger movements at different speeds also indicate that muscle activity is needed both for producing motion at joints and to counteract dynamic inertial torque (14).

Modeling of hand function, in a person with tetraplegia, needs to account for both altered physical characteristics of the hand and the potential treatment modalities that could be applied to improve function. Typically, after a high spinal cord injury, the hand is transformed into a more flexed posture than normal, where passive joint moments can represent a major part of the total joint moment. Muscle strength in people using functional neuromuscular stimulation systems may be reduced up to 80% when compared with a normal hand (22). Finally, treatment modalities such as joint fusion and tendon transfers should be included in a model of the hand.

The purpose of this study was to develop a dynamic model of the hand and to use this model for evaluating the function that could be obtained in people with tetraplegia using functional neuromuscular stimulation. This model is distinct, with respect to other dynamic models of hand function, in that it includes the unique characteristics of the hand of a person with tetraplegia and treatment modalities used to improve function in such cases.

METHODS

The hand was modeled as a multibody system connected by moveable joints. Each joint was subjected to active, passive, and external moments. Active joint mo-

Acknowledgment—This work was supported by the Neural Prosthesis Program of the National Institute of Neurological Diseases and Stroke under Contract N01-NS-2-2344.

Address correspondence to Joseph M. Mansour, Department of Mechanical and Aerospace Engineering, Case Western Reserve University, Cleveland, OH 44106, U.S.A.

(Received 5Oct95, Revised 17May96, Revised 6Aug96, Accepted 3Jul96)

ment arises from contraction of muscles crossing joints. Passive moment represents the resistance of a joint to movement, when all muscles are inactive. External moment is the result of contact forces between the hand segments and a grasped object. The complete model of hand function was built around the program ADAMS (Mechanical Dynamics, Inc., Ann Arbor, MI, USA).

Thumb, index finger, palm, and intersegmental joints were included in the model. The plane of the palm was fixed and parallel to the gravitational direction. Each phalanx was represented by a cylindrical rigid body whose dimensions were measured on one subject. Segment masses and principal moments of inertia were computed based on the volume and geometry of each segment, using a specific mass of 1.1 g/cm^3. The index finger and thumb articulations were modeled as 1 or 2 degree-of-freedom joints (Table 1).

Fifteen muscle-tendon units were included in the hand model (Table 2). These muscles were selected because they are typically used in upper extremity functional electrical stimulation systems at our institution. The force in each muscle was a function of its activation dynamics, length-tension-firing period and force-velocity properties (Appendix). Passive properties of the muscles were included in the passive moments. By scaling slow-twitch human soleus data from Bawa and Stein (5) to a fast muscle response (32), the activation time constant was estimated to be 33 msec. Parameters for the normalized length-tension-firing period and force-velocity relationships were based on measurements for cat soleus (13), but were adjusted for the correct physiological length range (10) for each muscle (Table 2). Peak isometric force was estimated from measured physiological cross-sectional area (3) and maximum specific muscle stress, 20 N/cm^2 (9). Muscle geometric parameters were generally taken from the literature (23), but when not available, were estimated *in vivo* from measurements on the surface of a subject's arm. The firing period of motor neurons was assumed constant (80 msec), but activation was varied as a function of time (10). Moment of muscle force was computed using a constant moment arm (4) for all muscles except the oblique and transverse heads of adductor pollicis, and the transverse head of the dorsal interosseous (Table 3). For these three intrinsic muscles, joint moment was the product of muscle force applied along a straight line between the origin and the insertion points of the muscle, and the moment arm was the computed perpendicular distance between a joint and the muscle force.

The contact force was computed as that needed to produce deformation of the finger resulting from its intersection with an object and be in equilibrium with all other forces. The constitutive response of finger pads was obtained from a series of force and displacement measurements (17). These data were fit to a model of the form

$$\begin{aligned} F_n &= f_1(d) + f_2(d) \cdot (d)^r \\ f_1 &= \frac{f_l + f_u}{2} \\ f_2 &= \frac{f_l - f_u}{2} \\ f_l &= a_l e^{b_l d}, f_u = a_u e^{b_u d}, \end{aligned} \tag{1}$$

where F_n is the perpendicular component of the external force, d is the magnitude and $\dot{d}$ is the velocity of penetration of an object into a finger segment, r was estimated as 0.1 (16), and f_l and f_u represent the loading and unloading branches of the finger pad force-displacement relationship that were fit by exponential functions (Table 4). The magnitude and velocity of penetration of a hand segment by an object, perpendicular to the contact surface, were computed from the kinematics of the hand-object interaction (15).

The tangential component of the contact force, $\mathbf{F}_t$, was computed using the perpendicular force, F_n, and a constant coefficient of friction ($\mu = 0.5$) representing contact between finger and a polished surface (29). The tangential force was applied in a direction opposite to the tangential velocity of the segment with respect to the object (15)

$$\mathbf{F}_t = -\mu F_n \hat{\mathbf{v}} \tag{2}$$

where $\hat{\mathbf{v}}$ is a unit vector in the direction of the relative tangential velocity. Frictional forces are discontinuous, resulting in a failure of the integration, in a simulation, to converge. To improve convergence, the discontinuity in

TABLE 1. Degrees of freedom of joints in the hand model taken from An *et al.* (2), Cooney *et al.* (12), and Toft and Berme (27).

Model Element	Joint	Mechanical Equivalent	Degrees of Freedom
Thumb	Carpometacarpal	Universal joint	2
	Metacarpophalangeal	Revolute joint	1
	Interphalangeal	Revolute joint	1
Index Finger	Metacarpophalangeal	Universal joint	2
	Proximal interphalangeal	Revolute joint	1
	Distal interphalangeal	Revolute joint	1

TABLE 2. Parameters and computed forces of the muscles in the model (see Appendix).

Muscle	Length-Tension Parameters		Force-Velocity Parameter	Computed Forces	
	$a \times 10^{-4}$ (1/sec)	$b \times 10^{-3}$ (1/cm · sec)	C (1/cm)	F_0 (N)	F_{iso} (N)
Flexor digitorum profundus*	1.0	0.895	0.012	82	57.9
Flexor digitorum superficialis*	1.0	1.054	0.014	72	60.9
Extensor indicis*	1.0	1.342	0.018	22	13.7
Extensor digitorum communis*	1.0	0.984	0.013	22	13.8
First palmar interosseous	1.0	3.75	0.050	28	19.2
First dorsal interosseous, parallel head	1.0	7.5	0.010	28	19.5
Flexor pollicis longus*	1.0	1.41	0.019	102	81.9
Flexor pollicis brevis	1.0	24.19	0.333	46	27.7
Extensor pollicis longus*	1.0	1.28	0.017	38	22.7
Extensor pollicus brevis	1.0	1.84	0.024	26	19.9
Abductor pollicis longus*	1.0	3.750	0.050	78	65.5
Abductor pollicis brevis	1.0	25.0	0.333	30	17.3
Adductor pollicis, oblique head	1.0	3.0	033	48	45.2
Adductor pollicis, transverse head	1.0	3.0	0.028	18	17.1
First dorsal interosseous, transverse head	1.0	2.14	0.028	42	40.2

The isometric muscle force was computed with all joints fixed at 0°. Length of the muscles indicated by an asterisk is taken from Lieber *et al.* (23). For the rest of the muscles, muscle length was measured *in vivo*.

the friction was approximated by a piecewise continuous function, using the ADAMS "STEP" subroutine, and a threshold velocity (0.01 cm/sec) was set such that there was always relative motion between contacting surfaces.

TABLE 3. Tendon moment arms at the joints of the thumb and index finger.

Muscle	Thumb Moment Arms (cm)			
	CMC (Flx)	CMC (Add)	MP (Flx)	IP (Flx)
FPL	0.83	0.85	1.0	0.98
FPB	1.87	0.78	1.0	0
EPL	−1.37	0.25	−1.07	−0.65
EPB	−0.84	−0.95	−1.03	0
APL	0.47	−1.11	0	0
APB	1.46	−0.50	1.32	0

Muscle	Index Finger Moment Arms (cm)			
	MCP (Flx)	MCP (Add)	PIP (Flx)	DIP (Flx)
FDP	1.11	0.11	0.79	0.41
FDS	1.19	0.17	0.62	0
EI	−0.90	0.13	−0.27	−0.21
EDC	−0.86	−0.02	−0.27	−0.21
PI1	0.66	0.58	−0.26	−0.16
$DI1_p$	0.37	−0.61	0	0

Flexion (Flx) and adduction (Add) are the positive directions. CMC, carpometacarpal; MP, metacarpophalangeal; IP, interphalangeal; FPL, flexor pollicis longus; FPB, flexor pollicis brevis; EPB, extensor pollicis brevis; APL, abductor pollicis longus; APB, abductor pollicis brevis; MCP, metacarpophalangeal; PIP, proximal interphalangeal; DIP, distal interphalangeal; FDP, flexor digitorum profundus; FDS, flexor digitorum superficialis; EI, extensor indicis; EDC, extensor digitorum communis; PI1, first palmar interosseous; $DI1_p$, first dorsal interosseous, parallel head.

To aid in specifying muscle activation patterns, the hand model was interfaced with optimization software (DOT and DOC; VMA Engineering) that minimized the difference between either the current, and the desired joint positions, or total grasp force (Fig. 1),

$$\text{Minimize:} \quad OBJ = \sum_{j=1}^{m} [T_j - \Theta_j(\alpha_1, \ldots, \alpha_n)]^2, \tag{3}$$

for position optimization, or for force optimization

$$\text{Minimize:} \quad OBJ = [F_d - f(\alpha_1, \ldots, \alpha_n)]^2, \tag{4}$$

where the constraints in both cases are

$$0 \leq \alpha_1 \leq 1, \quad 0 \leq \alpha_2 \leq 1, \quad \ldots, \quad 0 \leq \alpha_n \leq 1. \tag{5}$$

In these equations, T_j is the desired joint position at the jth joint, m is the number of joints, Θ_j is the current joint

TABLE 4. Coefficients of regression of the loading and unloading force-displacement curves of the web space thumb, and index finger pads (15).

Finger Pad	Coefficients of Regression $f_l = a_l e^{b_l d}$, $f_u = a_u e^{b_u d}$					
	a_l (N)	b_l	r^2	a_u (N)	b_u	r^2
Web	0.06	7.0	—	0.02	8.0	—
TPP	0.078	9.225	0.953	0.0231	10.003	0.961
TDP	0.0599	8.395	0.993	0.0218	8.803	0.980
IPP	0.0337	10.247	0.980	0.0030	12.414	0.980
IMP	0.0689	12.217	0.956	0.0134	14.480	0.978
IDP	0.0503	15.029	0.924	0.0094	17.330	0.965

The coefficients for the web space are estimated from the coefficients of the finger pads. TPP, thumb proximal plalanx; TDP, thumb distal phalanx; IPP, index proximal phalanx; IMP, index middle phalanx; and IDP, index distal phalanx.

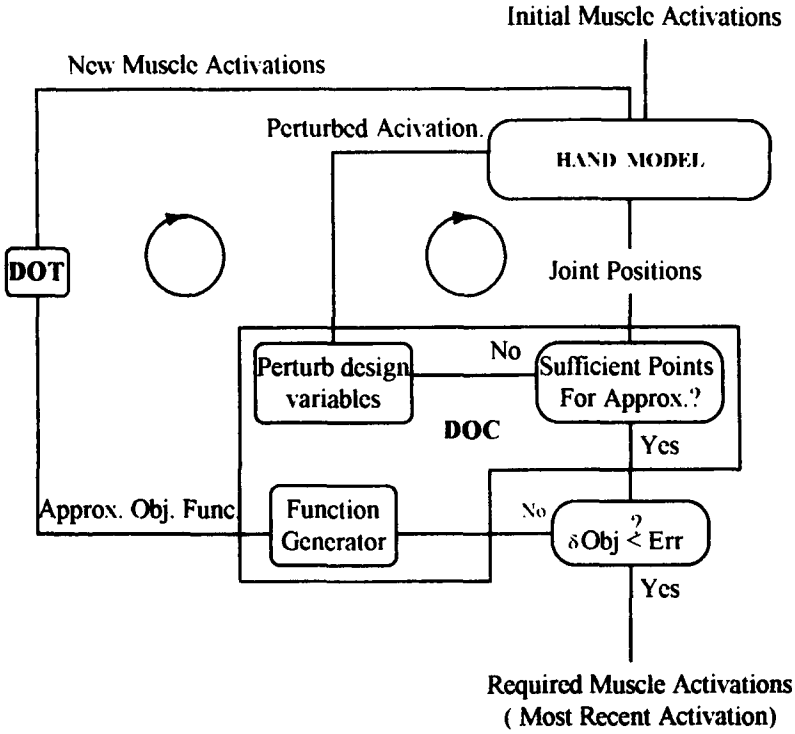

FIGURE 1. Schematic of the interface between the hand model implemented in ADAMS and the optimization routines. Optimization routines control neural inputs to move the joints into the desired positions by minimizing the differences between the initial and the desired joint angles.

angle, F_d is the total desired grasp force, f is the current grasp force, and α_i are the activation parameters for each of the n muscles in the model. The activation parameters are scaled from zero for no activation to one for full activation (10).

Because active muscle forces may be much less in people using functional neuromuscular stimulation, than in volitionally controlled muscles (22), the upper limits of <1 for muscle activation was imposed in some simulations. Moreover, to represent the hand of a person with tetraplegia, passive moment was measured at the metacarpophalangeal joint of a tetraplegic patient (Fig. 2). Passive moment at the index finger interphalangeal joint of a person with tetraplegia was estimated from measurements on a normal subject, which were modified based on joint range of motion, and rest position that specifies the angle where passive moment is 0.

The sensitivity of joint position to muscle activation was evaluated by activating muscles individually, in 10 steps, from 0 to 100%, and computing the resulting joint positions. Muscles that produced the greatest joint rotation, for an increment of activation, were ranked as most effective. These results were used to select primary muscles for a specific task.

When possible, model predictions were compared with results in the literature. Maximum isometric force predicted by the model was compared with data given by Ketchum and Thompson (18). Muscle activation in reciprocal posture was compared with electromyographic results (24). Predicted lateral grasp force was compared with experimental results (2,20). Finally, a dynamic interaction response of the index finger, observed by Darling and Cole (14), was simulated using the model.

Two tip pinch positions, corresponding to thick and thin objects (Table 5, Cases 1 to 6), and reciprocal movement, corresponding to a terminal position of metacarpophalangeal flexion and interphalangeal extension, were simulated (Table 5, Cases 7 to 13). The flexor digitorum superficialis, extensor indicis, extensor digitorum commu-

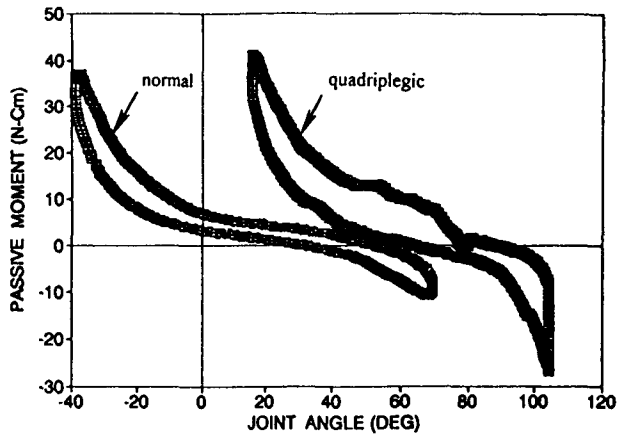

FIGURE 2. Passive moment hysteresis loop at the metacarpophalangeal joint of a normal subject (J.M.) and a tetraplegic person (K.T.). The horizontal arm of the apparatus could not be rotated >105° of flexion; therefore, for Subject K.T., data are not recorded beyond that point.

TABLE 5. Summary of the simulations of index finger function in tip pinch of thin (cases 1 to 3) and thick (cases 4 to 6) objects and reciprocal motion (cases 7 to 13).

Case #	Desired Posture (Degrees of Flx)	Passive Moment (Rest Position)	Tendon Transfer	Activation Limits
1	θ^{MCP} = 40,	Normal		
2	θ^{PIP} = 45,	Intermediate		
3	and θ^{DIP} = 15	High		
4	θ^{MCP} = 20,	Normal		
5	θ^{PIP} = 25,	Intermediate	None	$0 \leq \mu \leq 100\%$
6	and θ^{DIP} = 15	High		
7		Normal		
8		Intermediate		
9	θ^{MCP} = 90,	High		
10	θ^{PIP} = 0,	Normal	Zancolli-lasso	
11	and θ^{DIP} = 0	High	Zancolli-lasso	$0 \leq \mu \leq 40\%$
12		Normal	Intrinsicplasty	
13		High	Intrinsicplasty	

Passive moments were based on a normal hand (normal) and extreme case from the hand of person with tetraplegia (high, as in Fig. 2), and an intermediate case between normal and high stiffness. Flx, flexion; MCP, metacarpophalangeal; PIP, proximal interphalangeal; DIP, distal interphalangeal.

nis, and first palmar interosseous were used in these simulations. A range of passive moments, muscle strengths, and the effect of two tendon transfers [a Zancolli-lasso (33) and an intrinsicplasty] was studied. The Zancolli-lasso was modeled by eliminating the moment of the flexor digitorum superficialis at the proximal interphalangeal joint. The intrinsicplasty was modeled by applying flexor digitorum superficialis force with the extensor mechanism moment arm at the interphalangeal joints. In all simulations, the thumb was abducted from its rest position by activation of abductor pollicis longus.

The function of the thumb in lateral pinch was modeled assuming that the thumb contacted an object that had a flat surface (coefficient of friction 0.5), was perpendicular to the gravitational direction, and was fixed to the ground. Moreover, it was assumed that the shape of the contacting surface of the thumb was a sector of a sphere and that only the distal phalanx of the thumb was in contact with the object. From a preliminary study (15), the center of the sphere was located at 1.3 ± 0.2 cm parallel to the phalanx and 1.55 ± 0.2 cm perpendicular to the palmar surface of the phalanx, with respect to the center of the interphalangeal joint. The radius of the sphere was 2.8 ± 0.3 cm. An implementation of lateral pinch in people using functional neuromuscular stimulation was simulated: the interphalangeal joint is fused and the adductor pollicis, or the flexor

TABLE 6. Dynamic simulations are performed using a variety of object sizes, masses, and initial positions and two levels of maximum muscle strength.

Case No.	Maximum Activation Limit (%)	Diameter (cm)	Mass (kg)	Initial Position (cm) X	Initial Position (cm) Y	Required Force (N)	EI Activation (%)
1				9.5	3.8		8.0
2		4.0	0.3	13.5	3.8	2.1	25.0
3				16.5	3.8		48.0
4	100	6.0	0.9	10.5	4.8	6.3	18.0
5		6.0	0.9	14.5	4.8	6.3	35.0
6		8.0	1.8	11.5	5.8	12.6	18.0
7	40	6.0	0.9	10.5	4.8	6.3	18.0
8	40	6.0	0.9	14.5	4.8	6.3	35.0

Position of center of mass of the object is given relative to the center of rotation of the wrist. The required normal force is computed from Eq. 4. Before dynamic simulations, the index finger is positioned close to the object, by activation of the extensor indicis (EI).

TABLE 7. Comparison of the maximum isometric force of the index finger muscles predicted by our model and measured by Ketchum and Thompson (18) on live subjects.

	Maximum Muscle Isometric Force (N)	
Muscle	Our Model	Ketchum and Thompson
FDP	57.9	60.6 ± 25.9
FDS	60.9	67.8 ± 23.2
Extensor	27.5	58.7 ± 28.1
PI1	19.2	27.2 ± 11.5
DI1	19.5	53.4 ± 24.7

FDP, flexor digitorum profundus; FDS, flexor digitorum superficialis; PI1, first palmar interosseous; DI1p, first dorsal interosseous.

pollicis longus, is activated (20). The effect of fusion angle on hand function was evaluated. In addition, alternatives that do not rely on joint fusion were investigated.

Palmar grasp of cylindrical objects of several diameters and weights, with normal and weak muscles (Table 6), and with the object either fixed to the ground or free to slide on a horizontal flat plane with friction, were modeled. Phalanx-object interaction was computed from the intersection of two cylinders, whereas that of web space and object was modeled as the intersection of a straight line and a cylinder (15). Before each grasp and hold simulation, the thumb was extended and abducted using extensor pollicis brevis and abductor pollicis brevis, and the index finger was extended using extensor indicis. To determine a muscle activation pattern for a dynamic grasp of a moveable object, the object was first fixed, and in contact with the proximal phalanx of the thumb and the web space: its approximate final position. Force optimization, Eq. 4, was used to search for the activation of flexor digitorum profundus and flexor digitorum superficialis to provide the force needed to hold an object against gravity by frictional forces. The required normal force, N, on the object was found by noting that support forces are equally shared by the thumb and the fingers, and the force is equally shared between the index and other fingers, and the actual support force is ~40% greater than this (1,26,30),

$$1.4\left(\frac{W}{4}\right) = \mu N, \tag{6}$$

where the coefficient of friction, μ, was 0.5 (29).

RESULTS

The sensitivity analysis ranks flexor digitorum superficialis, flexor digitorum profundus, first palmar interosseous, and first dorsal interosseous as the most to least effective flexors of metacarpophalangeal joint of the index finger. Except for first dorsal interosseous, which significantly abducts metacarpophalangeal joint, other muscles produce adduction. At the proximal interphalangeal joint, flexor digitorum profundus and flexor digitorum superficialis produce flexion; first dorsal interosseous has no effect; and extensor indicis, extensor digitorum communis and first palmar interosseous provide similar small extension. At the distal interphalangeal joint, only flexor digitorum profundus produces flexion. In extension, extensor indicis and extensor digitorum communis have almost the same effect at all the index finger joints. Flexor pollicis longus and brevis, and abductor pollicis longus and brevis flex the carpometacarpal joint, with the former being the most effective and the latter being the least effective. Extensor pollicis longus is more effective than extensor pollicis brevis in extending the carpometacarpal joint. None of the intrinsic thumb muscles, except adductor pollicis (oblique head), which flexes carpometacarpal joint, have a significant flexion/extension effect at carpometacarpal joint. Flexor pollicis longus, adductor pollicis (oblique head), flexor pollicis brevis, and abductor pollicis brevis are, respectively, the strongest flexors of the thumb metacarpophalangeal joint, whereas extension of the joint is fulfilled by extensor pollicis longus and extensor pollicis brevis. At the interphalangeal joint, flexor pollicis longus is a strong flexor, and extensor pollicis longus is a weak extensor.

From a series of static simulations, the maximum isometric force, predicted by the model, for the flexor digitorum profundus, flexor digitorum superficialis, and first palmar interosseous are in good agreement with experimental measurements (18). However, the model predicts lower forces for the extensor and first dorsal interosseous (Table 7). A dynamic simulation of activation of the flexor digitorum superficialis shows, qualitatively, the same results reported by Darling and Cole (14): initial metacarpophalangeal joint extension and proximal interphalangeal joint flexion.

Simulations show that positioning the finger in a tip pinch posture depends on the combined influences of passive moments at the joints, muscle strength, and the specific posture. A tip pinch posture, suitable for grasping a thin object, can be obtained with relatively low activation, even in hands with elevated passive moments (Tables 5 and 8; Fig. 3). In contrast, tip pinch of a thick object requires much greater activation. Although individual joint angles may be far from the desired values, the overall posture is still functional (Tables 5 and 8; Fig. 4). The muscle activation pattern selected by the optimization in tip pinch of a thick object is in agreement with electromyographic recordings (24), in the sense that extrinsics alone produce clawing and action of intrinsics is required.

The desired end-point joint angles for a reciprocal movement of the finger are unreachable by activation of the extrinsic muscles, flexor digitorum superficialis, extensor indicis, and extensor digitorum communis alone (Table 8). With the intrinsic first palmar interosseous fully

TABLE 8. Minimum required activation of the selected muscles and the resultant postures for different cases simulated (Table 5).

Case No.	Minimum Required Activity (%)				Obtained Posture (°)		
	FDS	EI	EDC	PII	θ^{MCP}	θ^{PIP}	θ^{DIP}
1	0	0	0	0	41	42	22
2	0	14	0	0	36	60	17
3	0	52	0	15	34	64	12
4	—	20	0	0	18	37	18
5	—	100	7	23	2	48	5
6	—	100	75	30	13	56	2
7	0	10	0	100	76	24	14
8	0	75	0	100	62	44	4
9	0	94	0	100	68	58	4
10	30	40	—	—	78	26	11
11	18	40	—	—	98	70	32
12	40	40	—	—	83	15	3
13	25	40	—	—	110	60	25

Dash (—) denotes that the muscle was not used in the simulation. FDS, flexor digitorum superficialis; EI, extensor indicis; EDC, extensor digitorum communis; PI1, first palmar interosseous; MCP, metacarpophalangeal; PIP, proximal interphalangeal; DIP, distal interphalangeal.

activated, joint angles close to the desired end-point posture are obtained (Fig. 5). The position of a finger with normal joint passive moments is the closest to the desired reciprocal posture, whereas a clawed hand is the farthest. Intrinsicplasty did not provide a good substitute for the first palmar interosseous in a clawed hand, because its flexion effect at metacarpophalangeal joint dominates its extension effect at proximal interphalangeal joint.

Simulations of lateral pinch show that when either adductor pollicis or flexor pollicis longus is fully stimulated, and the distal segment of the thumb contacts the radial side of the index finger, the resulting interphalangeal joint extension moment must be resisted by the passive moment or joint fusion. Increasing interphalangeal joint fusion angle decreases the normal component of the grasp force. A possible alternative pattern of muscle activation in lateral pinch is identified using the model. Full activation of adductor pollicis and abductor pollicis brevis, along with partial stimulation of flexor pollicis longus (30%), provides a functional posture for lateral pinch, and stabilizes the interphalangeal joint, without joint fusion or relying on the passive moment to prevent hyperextension (Fig. 6). In addition, the grip force produced by the alternative approach (17 N) is ~70% larger than the force produced with the current strategy (10 N).

Simulations of palmar grasp of a fixed, cylindrical object, supported by the thumb, shows a strong interaction of muscle strength and size of the object. A hand with weak muscles (40% activation), using only flexor digitorum superficialis and flexor digitorum profundus, cannot hold a 1.8 kg object (Tables 6 and 9), whereas a hand with full strength muscles can. As the weight of the object increases, the required activation level increases, whereas the activation level decreases when the size of the object increases. In other words, because muscle force is length-dependent, a large diameter object, for any weight, requires less muscle activation, than a small diameter object of the same weight, assuming we are on the ascending potion of the muscle length-tension curve.

In cases where the object is allowed to slide, it can be grasped successfully if it is initially positioned properly with respect to the hand (Table 10). When a relatively small object (4 cm diameter) is placed close to the tip of the index finger, the tip of the distal phalanx, rather than its palmar surface, contacts the object resulting in an unsuccessful palmar grasp: the object is not surrounded by the finger. The transition motion of the object from its initial to final position, in almost all of the cases simulated,

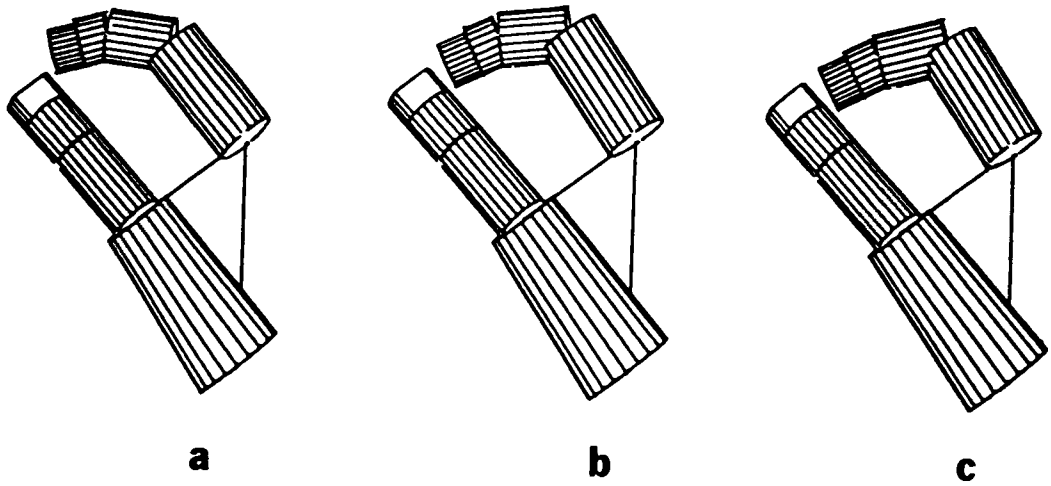

FIGURE 3. Best possible posture to pinch a thin object for a hand with (a) normal, (b) intermediate, and (c) high passive joint moments.

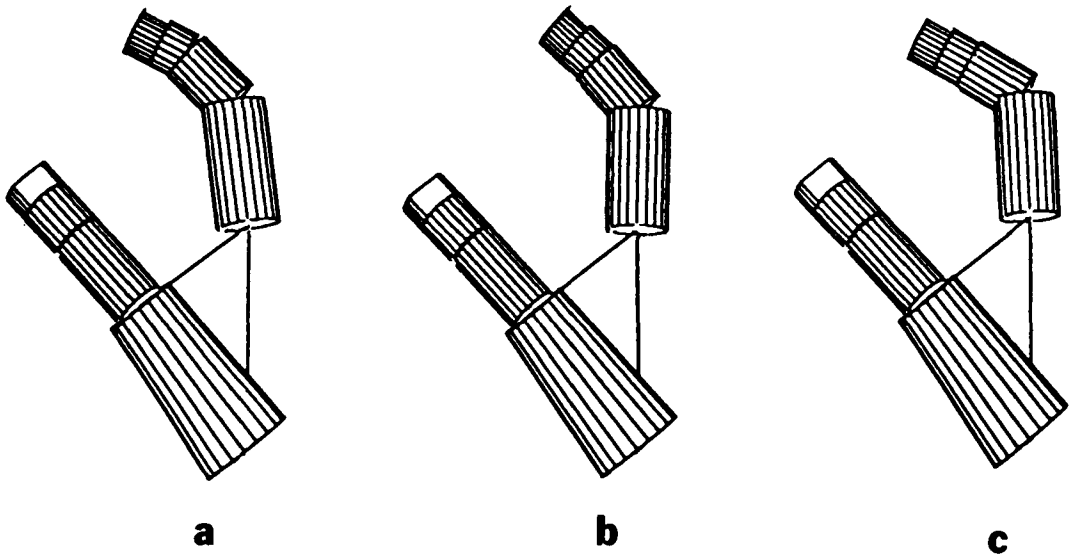

FIGURE 4. Best possible posture to pinch a cylinder with 5-cm diameter for a hand with (a) normal, (b) intermediate, and (c) high passive joint moments.

shows that by activation of the flexor digitorum superficialis, the object is dragged into the palm and is entrapped, and by activation of flexor digitorum profundus, sufficient force to hold the object is provided (Fig. 7).

DISCUSSION

A three-dimensional dynamic model of the thumb and the index finger was developed and implemented. The model was used to investigate hand performance in tip pinch, lateral pinch, and palmar grasp with specific application to people with tetraplegia using functional neuromuscular stimulation. It was shown that combinations of weak muscles and abnormally high passive moment, associated with clawed or overly flexed index finger joints, may prevent the digits from reaching certain postures, even with the help of common tendon transfer techniques. Simulations of lateral prehension revealed that an alternative approach, to the strategy currently used in functional neuromuscular stimulation, may also provide functional lateral pinch. Simulations of palmar grasp disclosed that extrinsic muscles might be sufficient to grasp and hold cylindrical, movable objects, if before the grasp, an open posture is achieved, and the object is placed as close as possible to the palm. However, sufficient extension of the proximal interphalangeal joint, to permit hand opening, may be hindered by one, or a combination of, inadequate intrinsic muscle function, and increased passive moment.

Our model performs kinematic, static, or dynamic simulations in contrast to other models that generally perform only one type of simulation. In addition, several new features were incorporated into the model to meet our ultimate goal of improving hand function in people with tetraplegia. A dynamic model of muscle is used to drive the digits. This is essential, because we are interested in studying the effects of tendon transfers, joint fusion, and other procedures that alter muscle length and therefore force. The model also includes dynamic joint passive moment that seems to be needed to ensure joint stability (22,31). Dynamic simulation of grasp is performed using index finger and thumb with rate-dependent models of finger pad deformation and frictional contact forces between fingers and objects. Joints were assigned degrees of freedom consistent with previous work (2,12), but modeling the thumb metacarpophalangeal joint is controversial (27). Because, for many applications of grasp, using functional electrical stimulation, the thumb is simply extended

TABLE 9. Minimum activation of the selected muscles required to produce adequate normal force to hold a fixed cylindrical object in palmar grasp with variety of object sizes and masses, and two levels of maximum muscle strength.

Object's Diameter (cm)	Maximum Activation Limit (%)	Object Mass (kg)					
		Minimum Required Activation (%)					
		0.3		0.9		1.8	
		FDS	FDP	FDS	FDP	FDS	FDP
4.0	100	32.4	0	77.9	0	100	45.3
6.0		21.3	0	61.2	0	100	25.2
8.0		17.3	0	49.5	0	100	17.3
4.0	40	32.4	0	40	36.9	Not	
6.0		21.3	0	40	22.2	sufficient	
8.0		17.3	0	40	18.6	normal force	

FDS, flexor digitorum superficialis; FDP, flexor digitorum profundus.

TABLE 10. Results of dynamic simulations of palmar grasp with different object masses, sizes, and initial positions (Table 6).

Case No.	Maximum Activation Limit (%)	Muscle Activation (%)		Final Position (cm)		Grip Force (N)	Residual Moment (N-cm)
		FDS	FDP	X	Y		
1		32.4	0	8.0	4.5	3.6	1.0
2		32.4	0	8.0	4.4	3.7	0.8
3		32.4	0	Unsuccessful palmar grasp			
4	100	61.2	0	8.4	5.4	7.2	3.8
5		61.2	0	8.2	5.8	6.5	0.4
6		100	17.3	9.3	6.1	13.0	3.9
7	40	40	22.2	8.5	5.3	7.4	2.2
8	40	40	22.2	8.2	5.8	6.7	1.6

Muscle activation in each case is determined by the results of optimization (Table 9). In each case, the magnitude of the total residual moment produced about the center of mass of the object is recorded. FDS, flexor digitorum superficialis; FDP, flexor digitorum profundus.

and held as a post against which an object is pressed by the fingers, we assigned only a flexion-extension degree of freedom to this joint.

Modeling each of these features of hand function requires a large number of parameters, many of which are not known for a specific subject and must be estimated. Muscle moment arms were generally obtained from published values, which represent an average for a small number of subjects, but may not be representative of any one person. Moment arms in tendon transfer surgeries were estimates and, in the case of an intrinsicplasty, probably represent an upper bound. Passive moments were based on extensive measurements on a normal hand and limited measurements on a person with tetraplegia. Finger pad measurements were based on normal hands. Simulation results should be viewed as general trends, not being specific to any individual. Obtaining subject specific data is an important next step in making models clinically applicable.

Despite having to estimate and generalize many model parameters, several tests of the model established its reliability. Predicted isometric forces showed good agreement with *in vivo* experimental data (18) for the index finger extrinsic flexor muscles where *in vivo* isolation of flexor digitorum profundus and superficialis could be reliably accomplished. In contrast, predicted muscle forces in first palmar interosseous, first lumbrical, and the extensor mechanism were not in close agreement with *in vivo* measurements. For these muscles, which are cotendonous, isolation of individual muscles would not be expected to be as reliable like the flexors, thus causing the measured force to be an overestimate of the actual muscle force. Muscle physiological cross-sectional areas (Table 2) support the notion that Ketchum's measurements overestimate the maximum forces in the extensor mechanism and first dorsal interosseous. Furthermore, the cross-sectional areas we used (3) are about twice as large as those given by Lieber

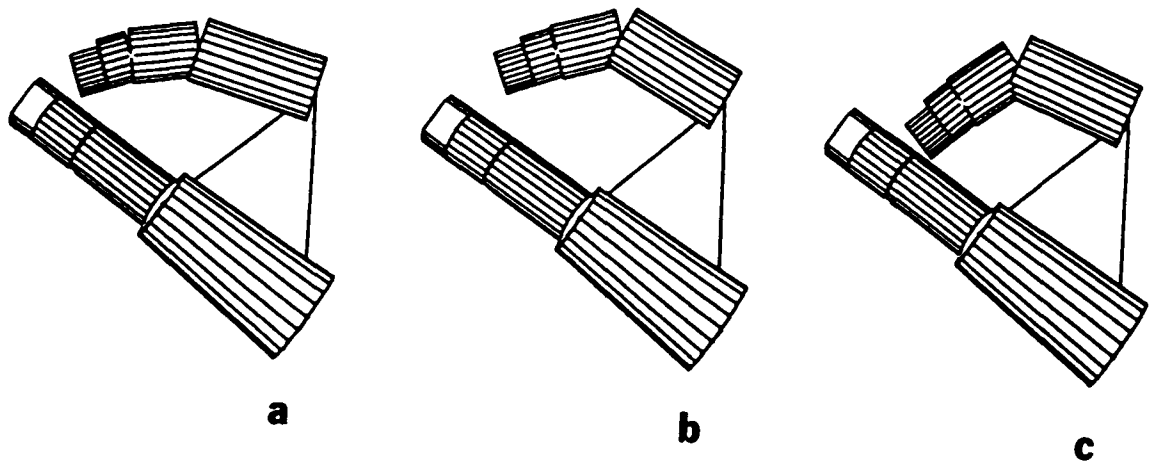

FIGURE 5. Best possible terminal posture of a reciprocal movement for a hand with (a) normal, (b) intermediate, and (c) high passive joint moments.

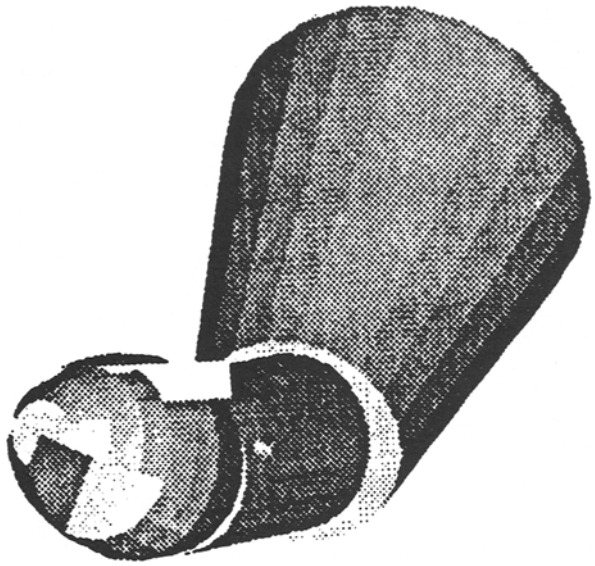

FIGURE 6. Front view (looking at the tip of the index finger when it is in zero position) of the thumb when the adductor pollicis and abductor pollicis brevis were fully and the flexor pollicis longus was partially (30%) activated. A functional lateral pinch posture was achieved. The normal force produced was 16.6 N.

et al., (23), thus suggesting that we are using estimates of the maximum isometric force that could already be high, yet these are less than those produced from *in vivo* measurements. Long (24) showed that, to reach or hold the index finger in a reciprocal position, intrinsic muscles, and (to a lesser extent) the extrinsic extensor mechanism are required. In our simulations, the optimization method chose to turn off the flexor digitorum superficialis, fully stimulate first dorsal interosseous, and partially activate extensor indicis, similar to electromyographic measurements. In simulations of lateral pinch, only selected muscles are stimulated, thus, it is not surprising that the predicted normal force is much <80 N measured in the normal hand (2). However, when adductor pollicis, first dorsal interosseous, first palmar interosseous, and part of flexor pollicis brevis were stimulated in people with tetraplegia (20), a pinch force of 9.7 ± 8.8 was obtained. Assuming that, in the adductor group, most of the normal pinch force is generated by adductor pollicis, this measurement is quite close to what our model predicts (7.5 N).

Both convergence and uniqueness were issues in optimizing hand function. Numerical convergence of the optimization, to yield muscle activation, was sensitive to the number of muscles included in the optimization. An initial attempt that included all 15 muscles, and allowed the optimization to select muscles needed for a specific task, did not converge, probably due to the redundancy of muscle action. The sensitivity analysis was then developed to determine which muscles produced the greatest change in objective for a given task, and a limited set of muscles was then used in the optimization with convergent results, but not necessarily unique results. Changing the initial position, in the optimization with a limited number of muscles, could result in a different set of muscle activation for the same final posture. This nonuniqueness is to be expected given the nonlinear and redundant nature of the system being studied.

Although, in the normal hand, joint angles converge close to desired postures, there are still differences between the desired and the final values of index finger joint angles (Table 8). This is entirely consistent with the posture of the subject whose passive moments were used in

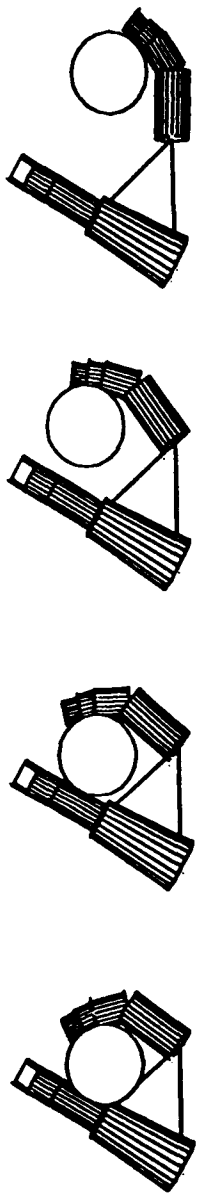

FIGURE 7. Case 5 (Table 5). The cylinder (diameter = 6.0 cm; mass = 0.9 kg) is successfully grasped between the index finger, thumb, and palm. Initial, final, and two intermediate pictures of the hand motion are presented.

the simulation. This subject (J.M.) has relatively stiff joints and cannot flex his metacarpophalangeal joint >80°, just as found in the simulation. A plot of the objective function showed that, at this simulated solution, a global minimum was obtained in the feasible space.

In summary, a reliable model of hand function was developed. Using the model, the complex interaction of all forces acting on the hand, and the effect of these forces on hand function, was evaluated. Passive joint moments, often neglected in many models of musculoskeletal function, were shown to be an important determinant of hand function in both palmar and lateral grasps.

REFERENCES

1. Amis, A. A. Variation of finger forces in maximal isometric grasp tests on a range of cylinder diameters. *J. Biomed. Eng.* 9:313–320, 1987.
2. An, K. N., E. Y. S. Chao, W. P. Cooney, and R. L. Linscheid. Forces in the normal and abnormal hand. *J. Orthop. Res.* 3: 202–211, 1985.
3. An, K. N., B. M. Kwak, E. Y. Chao, and B. F. Morrey. Determination of muscle and joint forces: a new technique to solve the indeterminate problem. *J. Biomech. Eng.* 106:364–367, 1984.
4. An, K. N., Y. Ueba, E. Y. S. Chao, W. P. Cooney, and R. L. Linscheid. Tendon excursion and moment arm of index finger muscles. *J. Biomech.* 16:419–425, 1983.
5. Bawa, P., and R. B. Stein. Frequency response of human soleus muscle. *J. Neurophys.* 39:78–793, 1976.
6. Biryukova, E. V., and V. Z. Yourovskaya. A model of human hand dynamics. In: Advances in the biomechanics of hand and wrist, edited by F. Schuind, K. An, W. P. Cooney, and M. Garcia-Elias. New York: Plenum Press, 1994, pp. 107–122.
7. Buchholz, B., and T. J. Armstrong. A kinematic model of the human hand to evaluate its prehensile capabilities. *J. Biomech.* 25:149–162, 1992.
8. Buchner, H. J., M. J. Hines, and H. Hemami. A dynamic model for finger interphalangeal coordination. *J. Biomech.* 21:459–468, 1988.
9. Burke, R. E., and P. Tsairis. Anatomy and innervation ratios in motor units to cat gastrocnemius. *J. Physiol.* 234:749–765, 1973.
10. Chiel, H. J., P. Crago, J. M. Mansour, and K. Hathi. Biomechanics of a muscular hydrostat: a model of lapping by a reptilian tongue. *Biol. Cybern.* 67:403–415, 1992.
11. Cole, K. J., and J. H. Abbs. Coordination of three-joint digit moments for rapid finger-thumb grasp. *J. Neurophys.* 55: 1407–1423, 1986.
12. Cooney, W. P., M. J. Lucca, E. Y. S. Chao, and R. L. Linscheid. The kinesiology of the thumb trapeziometacarpal joint. *J. Bone Joint Surg.* 63-A:1371–1381, 1981.
13. Crago, P.E. Muscle input/output model: the static dependence of force on length, recruitment and firing period. *IEEE Trans. Biomed. Eng.* 39:871–874, 1992.
14. Darling, W. G., and K. J. Cole. Muscle activation patterns and kinetics of human index finger movements. *J. Neurophys.* 63:1098–1108, 1990.
15. Esteki, A. Dynamic model of the hand with application in functional neuromuscular stimulation. Cleveland, OH: Department of Mechanical and Aerospace Engineering, Case Western Reserve University, Ph.D. Thesis, 1995.
16. Esteki A., and J. M. Mansour. An experimentally based nonlinear viscoelastic model of joint passive moment. *J. Biomech.* 29:443–450, 1996.
17. Hendrix, L. A., and J. M. Mansour. Functional grasp potential of the intrinsic minus hand. *IEEE Trans. Rehabil. Eng.* 1:145–153, 1993.
18. Ketchum, L. D., and D. E. Thompson. An experimental investigation into the forces internal to the human hand. In: Clinical mechanics of the hand, edited by P. W. Brand. St. Louis: The C. V. Mosby Co., 1985, pp. 325–331.
19. Keith, M. W., P. H. Peckham, G. B. Thrope, K. C. Stroh, B. Smith, J. R. Buckett, K. L. Kilgore, and J. W. Jatich. Implantable functional neuromuscular stimulation in the tetraplegic hand. *J. Hand Surg.* 14A:524–530, 1988.
20. Kilgore, K. L., P. H. Peckham, M. W. Keith, and G. B. Thrope. Electrode characterization for functional application to upper extremity FNS. *IEEE Trans. Biomed. Eng.* 37:12–21, 1988.
21. Leijnse J. N. A., C. J. Snijders, J. E. Bonte, J. M. F. Landsmeer, J. J. Kalker, J. C. Van Der Meulen, G. J. Sonneveld, and S. E. R. Hovius. The hand of the musician: the kinematics of the bidigital finger system with anatomical restrictions. J. Biomech. 26:1169–1179, 1993.
22. Lemay, M. Ph.D. Dissertation, Department of Biomedical Engineering, Case Western Reserve University, Cleveland, OH, 1994.
23. Lieber, R. L., B. M. Fazeli, and M. J. Botte. Architecture of selected muscles of the arm and forearm. *J. Hand Surg.* 17:804–809, 1992.
24. Long, C. Electromyographic studies of hand function. In: The hand, vol. I, edited by R. Tubiana. Philadelphia: W. B. Saunders Co., 1981, pp. 427–440.
25. Peckham, P. H., M. W. Keith, and A. A. Freehafer. Restoration of functional control by electrical stimulation in the upper extremity of the quadriplegic patient. *J. Bone Joint Surg.* 70-A:144–148, 1988.
26. Radwin, R. G., S. Oh, T. R. Jensen, and J. G. Webster. External finger forces in submaximal five-finger static pinch prehension. *Ergonomics* 35:275–288, 1992.
27. Toft, R., and N. Berme. A biomechanical analysis of the joints of the thumb. *J. Biomech.* 13:353–360, 1980.
28. Wells, R. P., D. A. Ranney, and A. Keller. The interaction of muscular and passive elastic forces during unloaded finger movements: a computer graphics model. In: Biomechanics. Current and interdisciplinary research, edited by S. M. Perren and E. Schneider. Dordrecht: Martinus Nighoff, 1985, pp. 743–748.
29. Westling, G., and R. S. Johansson. Coordination between grip force and vertical lifting force when lifting objects between index finger and thumb. *Soc. Neurosci. Abstr.* 7:247, 1981.
30. Westling, G., and R. S. Johansson. Factors influencing the force control during precision grip. *Exp. Brain Res.* 53:277–284, 1984.
31. Wu, C-H, J. C. Houk, K.-Y. Young, and L. E. Miller. Nonlinear damping of limb motion. Multiple muscle systems: biomechanics and movement organization, edited by J. M. Winters and S. L.-Y. Woo. New York: Springer-Verlag, 1990, pp. 214–235.
32. Zajac, F. E. Muscle and tendon: properties, models, scaling and application to biomechanics and motor control. In: CRC Critical Reviews in Biomedical Engineering, vol. 17, edited

by J. R. Bourne. Boca Raton, FL: CRC Press, 1989, pp. 359–411.
33. Zancolli, E. Structural and Dynamic Bases of Hand Surgery. Philadelphia: J. B. Lippincott Co., 1968, 198 pp.

APPENDIX

Muscle force was modeled as (10,13)

$$F_m = A(t)K_m(L_m - L_{ms})[1 + C\dot{L}_m] = A(t)F_0[1 + (a + b(L_m - L_{max}))T_F][1 + C\dot{L}_m], \quad \text{(A1)}$$

where muscle activation dynamics was modeled as a unity gain, linear first-order low pass filter:

$$\dot{A}(t) = p(\alpha - A(t)). \quad \text{(A2)}$$

Tendons were represented by linear springs with constant stiffness, in series with the muscle. Thus,

$$F_t = K_t(L_t - L_{ts}). \quad \text{(A3)}$$

The tendon and muscle length are related as

$$L_m + L_t = L_0 + \sum_{i=1}^{n} r_i \cdot \Theta_i, \quad \text{(A4)}$$

where the second term on the right-hand side of this equation represents the change in overall muscle-tendon length due to a change in joint angle from 0°. Substituting tendon length from Eq. A4 into Eq. A3, and recognizing that $F_m = F_t$, an expression for muscle length, independent of tendon length, was found. Substituting this expression for muscle length in Eq. (A1), an expression for computing muscle force was derived:

$$F_m = K[(L_0 + \sum_{i=1}^{n} r_i \cdot \Theta_i) - (L_{ms} + L_{ts})](1 + C\dot{L}_m) \quad \text{(A5)}$$

where

$$K = \frac{AK_mK_t}{AK_m(1 + C\dot{L}_m) + K_t}. \quad \text{(A6)}$$

NOMENCLATURE

$1/p$	= activation time constant of isometric force development
a,b	= muscle length-tension-firing period constants
n	= number of joints a muscle crosses
r_i	= tendon moment arm
A	= muscle activation
C	= muscle force-velocity constant
F_0, F_m	= peak isometric muscle force, muscle force
F_t	= tendon force
K_m	= muscle stiffness at the maximal recruitment level
K_t	= tendon stiffness
L_0	= muscle-tendon unit length when all joints are at 0°
L_m, L_{ms}, L_{max}	= muscle length, muscle slack length, maximum muscle length
L_t, L_{ts}	= tendon length, tendon slack length
T_F	= muscle firing period
α	= neural input
Θ_i	= joint angle